# Features of Diffusing Wave Spectroscopy

D. J. Pine,[*†] D. A. Weitz,[*] P. M. Chaikin,[*‡] and E. Herbolzheimer[*]

[*]*Exxon Research and Engineering, Annandale, New Jersey 08801*
[†]*Department of Physics, Haverford College, Haverford, Pennsylvania 19041*
[‡]*Department of Physics, Princeton University, Princeton, New Jersey 08540*

## Abstract

Photon correlation spectroscopy is extended to strongly multiply scattering systems by assuming that the transport of light is diffusive. A simple model is developed which accounts for different sample geometries, scattering configurations, absorption, and sample polydispersity. Experimental data are found to be in excellent agreement with the predictions. The dependence on geometry provides an important experimental control over the length and time scales probed.

## Introduction

Until recently the application of photon correlation spectroscopy (PCS) has been limited to the weak scattering regime, where only one scattering event occurs, and the scattering wavevector, $q$, is well determined. This has severely limited the utility of PCS either to very dilute systems or to systems which have been carefully index-matched to eliminate multiple scattering. However, many important practical applications of PCS involve optically dense systems in which multiple scattering is particularly wicked. In these cases, it is usually not possible to index-match the scatterers to their surroundings, and the interesting physics is lost upon dilution. While there have been several attempts to include multiple scattering events in the interpretation of PCS data, these have proven theoretically very difficult and have experimentally been limited to double or triple scattering. In this paper, we discuss a new technique which is explicitly applicable in the very strongly multiple scattering regime. We call this technique Diffusing Wave Spectroscopy.

The essence of this new technique is the diffusive nature of the transport of light in a strongly multiply scattering system. Recent work by Maret and Wolf (1) has shown how it is possible to exploit the diffusive nature of the transport to develop a theoretical framework for treating experimental results. Independently, Stephen (2) has derived theoretical expressions for the temporal autocorrelation functions of the scattered light. Here we develop a more physically transparent treatment of the method for interpreting experimentally measured autocorrelation functions from strongly multiply scattering systems. We show that the theoretical expressions derived are in excellent agreement with experimental results obtained from concentrated suspensions of polystyrene latex spheres. This now makes it possible to extend PCS to the multiple scattering regime. (3)

In the single scattering regime the length scale over which the dynamics are probed is determined solely by the $q$ vector and can be varied by using different scattering angles. This feature is lost in the multiple scattering regime, where the effect of many scattering events is to average over all accessible scattering vectors. Nevertheless, the autocorrelation functions are still very strongly dependent on geometry. However, using our approach, it is a simple matter to derive expressions for the autocorrelation functions in different experimental geometries.(3) Here we discuss two important experimental geometries, transmission and backscattering. Furthermore, we show how the geometry dependence can be exploited to probe the particle dynamics over vastly different length scales, and consequently over vastly different time scales. These features make DWS a potentially powerful and useful technique for studying the dynamics of optically dense systems.

## Theory

We begin by considering a relatively simple system which consists of a suspension of identical, noninteracting spherical scatterers with a diffusion coefficient, $D$. Following the analysis of Maret and Wolf, we consider a single light path which consists

of many scattering events, and calculate the decay in the autocorrelation function contributed by this path (1). The field autocorrelation function can be written as

$$G_1(\tau) = \langle E^*(0)E(\tau)\rangle \sim \left\langle e^{-i\Delta\phi(\tau)}\right\rangle \tag{1a}$$

where

$$\Delta\phi(\tau)= \sum_{i=1}^{n} q_i\cdot\Delta r_i(\tau) \tag{1b}$$

and where $q_i$ is the scattering wavevector of the $i^{th}$ scattering event, $\Delta r_i(\tau)=r_i(\tau)-r_i(0)$ is the change in position of the $i^{th}$ scattering particle in a time $\tau$, and $n$ is the number of scattering events in the path considered. By comparison, in single scattering, $\Delta\phi(\tau)=q\cdot\Delta r(\tau)$, and the autocorrelation function decays on a time scale given by $\Delta\phi\approx 1$. Similarly, in multiple scattering, the autocorrelation function will also decay when $\Delta\phi\approx 1$, but this will occur on a much shorter time scale because of the cumulative effect of the many scattering events.

We can evaluate the autocorrelation function for this path by first noting that the scattering events in the path are independent, so the average of the product of exponentials is the product of the average. Thus the autocorrelation function is

$$G_1(\tau) \approx \left\langle e^{iq\cdot\Delta r(\tau)}\right\rangle^n = \left\langle e^{-q^2\langle\Delta r^2(\tau)\rangle/6}\right\rangle^n$$

where the second equality follows from the independence of $q$ and $\Delta r$, allowing them to be averaged independently, and from the assumption that $\Delta r$ is a random Gaussian variable. We can perform the average over $q$ by keeping the first term of a cumulant expansion which gives

$$G_1(\tau) \approx e^{-\langle q^2\rangle\langle\Delta r^2(\tau)\rangle n/6}$$

where the approximation holds when $\langle q^2\rangle\langle\Delta r^2(\tau)\rangle n/6 \ll 1$. The average over $q$ in the exponential gives $\langle q^2\rangle = 2k_0^2(1-\langle\cos\theta\rangle)$, where the incident wavevector is $k_0=2\pi/\lambda$ with $\lambda$ the wavelength of the light in the medium. Here $\theta$ is the scattering angle and $\cos\theta$ is averaged over the form factor for a single sphere. It is convenient to introduce the transport mean free path, $\ell^*=\ell/(1-\langle\cos\theta\rangle)$, with $\ell$ the usual scattering mean free path. Thus,

$$G_1(\tau) \approx e^{-2Dk_0^2\tau(\ell/\ell^*)n}$$

where we have used the relation, $\langle\Delta r^2(\tau)\rangle = 6D\tau$, valid for simple diffusion.

Since there are many different paths the light can take, the total autocorrelation function is a sum over all the paths,

$$G_1(\tau) \propto \sum_{n=1}^{\infty} P(n)\, e^{-2(\tau/\tau_0)(\ell/\ell^*)n} \tag{2}$$

where $P(n)$ is the probability that the emerging light has scattered $n$ times in the sample and $\tau_0=1/Dk_0^2$. Since there is a of distribution paths with different $n$, we expect the autocorrelation function to be non-exponential.

The probability distribution $P(n)$ can in principle be determined by assuming that the transport of light through the sample consists of a random walk which is biased to account for anisotropy in scattering when the particle size is comparable to the wavelength of light. However, the problem of calculating $P(n)$ is greatly simplified by passing to the continuum limit, or diffusion approximation. This can be done by recognizing that the total path length traveled by light scattered $n$ times is given by $s=n\ell$. Then, substituting for $n$ and converting the sum in Eq. (2) to an integral over $s$ gives

$$G_1(\tau) \propto \int_0^{\infty} P(s)\, e^{-(2\tau/\tau_0)(s/\ell^*)}\, ds \tag{3}$$

where $P(s)$ is the probability that the light has travelled a path of length $s$ and $\tau_0=1/Dk_0^2$. It is interesting to note that the scattering mean free path, $\ell$, drops out of this expression (1). This arises from the fact that by passing to the continuum limit, we have effectively rescaled the random walk executed by light so that only one length scale appears in the problem, $\ell^*$, and on that length scale the random walk is isotropic. This is consistent with the diffusion approximation, where the sole length scale for the random walk is defined by the diffusion coefficient of light, $D_\ell=c\ell^*/3$, where $c$ is the speed of light.

To calculate $P(s)$, we can imagine an instantaneous pulse of light incident on the sample at time $t=0$ (3). If the light diffuses through the sample, there will be dispersion in the time dependence of the exiting pulse, reflecting the distribution of path lengths traversed by the light. Since $s=ct$, the probability that the light has traversed a path of length s is directly proportional to the intensity of the light exiting at time t. The exiting intensity is given by $\mathbf{n}\cdot\nabla U$ evaluated at the point where the light exits the sample, where n is a unit vector normal to the sample surface and U is the diffusing energy density inside the sample. The time evolution of U is described by the diffusion equation, $\partial U/\partial t = D_\ell\nabla^2 U$. This equation must be solved for the geometry appropriate for the particular experiment. We choose the simplest possible boundary conditions and set $U=0$ at all sample boundaries. To obtain the initial conditions, we assume that the light begins to diffuse a distance $z_0=\gamma\ell^*$ into the sample, where we expect that $\gamma\approx 1$. The transverse extent of the initial pulse is determined from the experimental

geometry by the width of the exciting laser beam. Thus $U_{in}(x,y,z,t)=\delta(z-z_0,t)$. The solution to Eq. (3) is simplified considerably by noting that $G_1(\tau)$ is the Laplace transform of $P(s)$ so that we can obtain the autocorrelation function directly from a solution of the Laplace transform of the diffusion equation. In fact, for most geometries of experimental importance, the solution to this diffusion equation can be found in standard texts (4).

**Transmission**

For a transmission experiment, we consider a slab of thickness $L$ and of infinite extent. For light incident from an extended plane source and collected from a point on the opposite side, we obtain

$$G_1(\tau) = \frac{L}{\gamma \ell^*} \sinh \gamma \sqrt{\frac{6\tau}{\tau_0}} \Big/ \sinh \frac{L}{\ell^*} \sqrt{\frac{6\tau}{\tau_0}}$$

$$\approx \frac{L}{\ell^*} \sqrt{\frac{6\tau}{\tau_0}} \Big/ \sinh \frac{L}{\ell^*} \sqrt{\frac{6\tau}{\tau_0}} \qquad (4)$$

where the second expression holds for $\tau \ll \tau_0$. By contrast, for light incident from a point source on axis with the detector we obtain,

$$G_1(\tau) \propto \int_{\sqrt{\frac{6\tau}{\tau_0}}\frac{L}{\ell^*}}^{\infty} \zeta \frac{\sinh \frac{\gamma \ell^*}{L} \zeta}{\sinh \zeta} d\zeta \qquad (5)$$

To compare these expressions with experimental data, we make use of the Seigert relation $G_2(\tau) = |G_1(\tau)|^2$.

We can gain physical insight into these equations by noting that the light must diffuse through the sample, introducing a characteristic path length, $s_c=n_c^*\ell^*$, where $n_c^*=(L/\ell^*)^2$ is the characteristic number of steps in a random walk of end-to-end distance $L$ with a step length $\ell^*$. Furthermore, since the autocorrelation function decays when $\Delta\phi\approx 1$, we can estimate the typical individual particle motion from the condition that $\langle\phi^2\rangle \approx k_0^2\langle\Delta r^2\rangle s_c/3\ell^* \sim 1$. This gives $\Delta r_{rms} \sim \lambda\ell^*/4L$. *Since $\ell^*/L \ll 1$, the typical particle motion probed by DWS in transmission is much smaller than the wavelength.* This reflects the fact that the decay of the autocorrelation function is due to the cumulative effect of many scattering events, so that the contribution to the total phase change due to individual particle motions is relatively small. *This is in striking contrast to ordinary PCS, where by varying q, length scales greater than or equal to the wavelength are probed.* Furthermore, the typical length scale of the particle motion probed by DWS in transmission can be varied simply by changing the sample thickness. In addition the characteristic time scales probed by DWS are considerably shorter than those probed by ordinary PCS, and are given by $\tau_0(\ell^*/L)^2 \ll \tau_0$. Finally we note that the experimental time scales ensure that the results are insensitive to $\gamma$, reflecting the fact that the details of the contribution of the first step are not important when the typical number of steps, $(L/\ell^*)^2 \gg 1$.

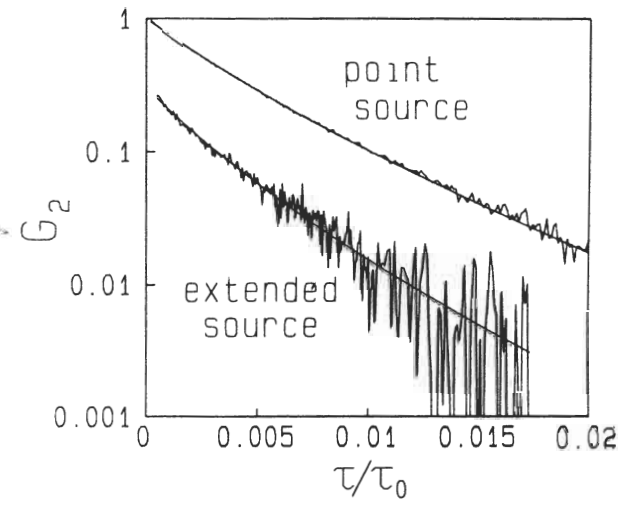


Figure 1. Intensity autocorrelation functions vs reduced time $\tau/\tau_0$ for transmission through 2–mm thick cells with 0.497–$\mu$m spheres and $\phi$=0.01.

To test the theoretical expressions derived above, we obtain homodyne autocorrelation functions using an aqueous suspension of 0.497-$\mu$m diameter polystyrene latex spheres at a volume fraction, $\phi$=0.01. One side of a 2–mm thick cuvette is uniformly illuminated by a 1–cm diameter beam from a 488 nm $Ar^+$ laser. Imaging optics are used to collect transmitted light from a 50-$\mu$m spot on the opposite side of the sample at the center of the illuminated area. A typical autocorrelation function obtained is shown in Fig. 1. The solid line through the data represents a fit using Eq. (4). Since $D$ is constant for $\phi \lesssim 0.01$, we use $\tau_0$=3.73 msec, as measured by PCS at very low volume fraction, and obtain $\ell^*$=144 $\mu$m from the fit to our data. If the excitation beam is focused to a point, on axis with the detected spot, the autocorrelation function decays somewhat more slowly, as shown in Fig. 1. Physically, this reflects the fact that there are fewer long paths when all the light emanates from a single point. However, using Eq. (5), we again obtain an excellent fit to the data and find $\ell^*$=143 $\mu$m. The excellent consistency between the two values for $\ell^*$ confirms that the different decay rates of the autocorrelation function are due solely to geometric effects.

The value of $\ell^*$ obtained from the dynamic measurements should be compared to those obtained from calculations using Mie theory (5, 6) and from static measurements of the enhancement in backscattered intensity at angles very near 180 degrees (7, 8). Both the calculations

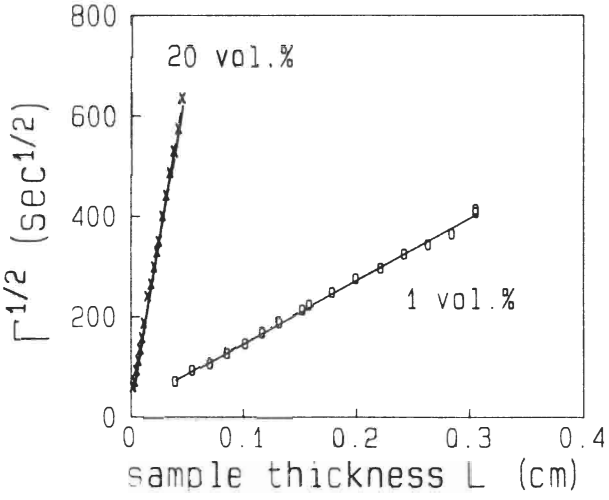


Figure 2. Square root of the first cumulant $\Gamma_1$ vs sample thickness $L$ for 0.497–$\mu$m spheres with $\phi$=0.01 and $\phi$=0.20.

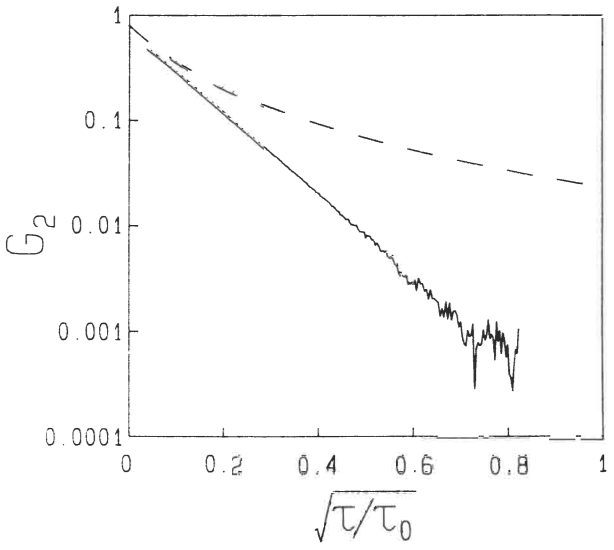


Figure 3. Intensity autocorrelation function vs square root reduced time for backscattering from a 1–mm thick cell with 0.497–$\mu$m spheres and $\phi$=0.05. The dashed line is $G_2(\tau) = |G_1(\tau)|^2$ from Eq. (9) with $\gamma$=2.

and the static measurements give values of $\ell^*$ about 30% larger than those obtained from DWS. We believe that the origin of this discrepancy is due at least in part to our use of overly simple approximations to the experimental boundary conditions for the diffusing intensity $U$. Instead of setting $U$=0 at the sample interface, a more realistic boundary condition would be to set $U$=0 a distance $\sim 2\ell^*/3$ outside the sample. Using the more realistic boundary conditions leads to closer agreement between the values of $\ell^*$ obtained from DWS and theory, but the experimentally obtained values are still 15% to 20% lower than the theoretical predictions. The origins of the remaining discrepancy remain unknown.

Despite the fact that paths of different lengths contribute to the decay of the autocorrelation function, the curvature is relatively small. This is due to the dominance of paths of a single length, $(L/\ell^*)^2\ell^*$, and it makes a cumulant analysis suitable. Indeed, short time expansions of Eqs. (4) and (5) reveal that the first cumulant of the autocorrelation function is $\Gamma_1 \propto (L/\ell^*)^2/\tau_0$. This provides a simple means of extracting the information from the data and again demonstrates the dependence of the decay rate on the sample thickness. Measurements of $\Gamma_1$ as a function of sample thickness are shown in Fig. 2 where we plot the square root of the first cumulant measured at different sample thicknesses and find the linear dependence expected. This is a convincing graphic illustration of the diffusive nature of the transport of light through the sample. In addition, it is apparent from Fig. 2 that the x–intercepts of the data occur not at the origin, but at $L \sim -4\ell^*/3$. This is consistent with the boundary conditions that $U$=0 a distance $2\ell^*/3$ outside the sample.

Finally, we find that the autocorrelation functions measured show no dependence on scattering angle or polarization, since any light transmitted through a sample has been scattered many times.

### Backscattering

For a backscattering experiment we again consider a slab of thickness $L$ and infinite extent. For light incident from an extended source and collected from a point on the same face, we obtain

$$G_1(\tau) = \frac{L}{1-\gamma\ell^*/L} \frac{\sinh\left[\sqrt{\frac{6\tau}{\tau_0}}\left(1-\frac{\gamma\ell^*}{L}\right)\right]}{\sinh\frac{L}{\ell^*}\sqrt{\frac{6\tau}{\tau_0}}}$$

$$\rightarrow \exp\left(-\gamma\sqrt{\frac{6\tau}{\tau_0}}\right), \text{ for } L \gg \ell^*. \qquad (6)$$

In the limit that $L \gg \ell^*$, $\ell^*$ drops out of the expression for the autocorrelation function, reflecting the fact that light paths of all length scales contribute to the decay. This broad distribution of path length leads to a broad distribution of time scales resulting in the stretched exponential form for $G_1(\tau)$.

To test the form of the autocorrelation function, we illuminate a 1 cm thick cuvette containing 0.497-$\mu$m diameter polystyrene latex spheres at $\phi$=0.05. The incident beam intensity is uniform over a 1-cm diameter spot size and the backscattered light is collected from a 50-$\mu$m point at

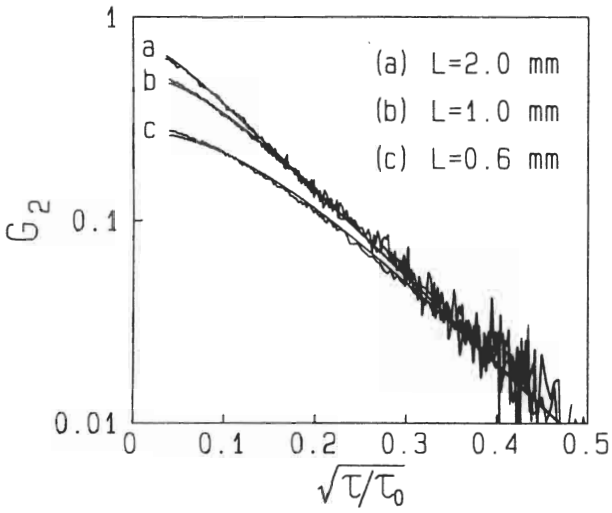


Figure 4. Intensity autocorrelation functions vs square root reduced time for backscattering from cells with different thicknesses $L$.

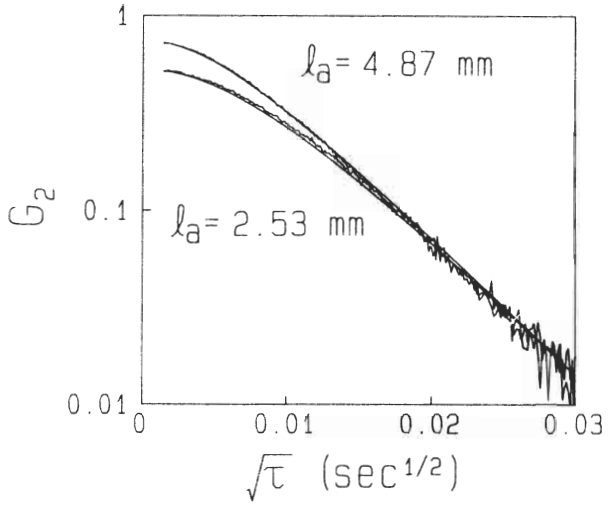


Figure 5. Intensity autocorrelation functions vs square root reduced time for backscattering from samples with absorbing dye in the suspending liquid.

the center. We use an analyzer to collect only the depolarized light thus ensuring multiple scattering. The autocorrelation function which results is shown in Fig. 3 where we have plotted the logarithm of $G_2$ as a function of the square root of the reduced time, $\tau/\tau_0$. The linear shape of this plot is striking evidence that the functional form correctly describes the data over nearly three decades of decay. If we again assume $\tau_0$=3.73 msec, the slope of the data in Fig. 3 gives $\gamma\approx 2$.

In principle, the initial slope of the autocorrelation function diverges, reflecting the contribution of infinitely long paths which decay infinitely rapidly. In practice, this divergence is cutoff by finite size effects within the sample, which limit the extent of the longest paths. This results in a corresponding rounding of the correlation function at times shorter than $\tau_0(\ell^*/R)^2$ where $R$ characterizes the finite extent of the longest paths which have a path length $(R/\ell^*)^2\ell^*$. The introduction of this new length scale will once again make the autocorrelation function dependent on $\ell^*$. In Fig. 3, the shortest delay time measured by the correlator is longer than any other cutoff times. However, such effects are often observed where $R$ is determined by the finite size of the exciting laser beam, the finite thickness of the sample, or a new length introduced by absorption in the sample.

Within our theoretical formalism, it is a simple matter to to account for these effects. As an example, in Fig. 4 we show autocorrelation functions obtained in backscattering for samples with different values of $L/\ell^*$. These are obtained using 0.497-$\mu$m diameter spheres with $\phi$=0.01, and with sample thicknesses of 0.6, 1.0, and 2.0 mm. The solid lines through the data are obtained from Eq. (6) using $\gamma$=2.0 measured for an thick sample at this volume fraction; $\tau_0$=3.73 msec measured with PCS in the single scattering limit; and $\ell^*$=144-$\mu$m from the DWS transmission measurements. Thus, other than an overall normalization, there are no adjustable parameters. The agreement between the data and theory is very good.

As a further example of how the initial infinite decay rate of the autocorrelation function can be cutoff, in Fig. 5 we show autocorrelation functions obtained in backscattering when an absorbing dye, methyl red, is added to the suspending liquid. These data are obtained using samples with 0.497-$\mu$m spheres at $\phi$=0.01 to which varying amounts of methyl red have been added. The absorbing dye preferentially cuts off long paths causing the autocorrelation functions to roll over at small times, as can been seen in Fig. 5. We can account for these data by introducing into Eq. (3) a factor which exponentially attenuates long paths:

$$G_1(\tau) \propto \int_0^\infty P(s) e^{-s/\ell_a} e^{-(2\tau/\tau_0)(s/\ell^*)}\, ds \qquad (7)$$

where $\ell_a$ is the absorption length due to the dye. Eq. (7) implies that autocorrelation functions obtained in the absence of absorption may be extended to account for absorption by replacing $2\tau/\tau_0$ in Eq. (3) by $2\tau/\tau_0+\ell_a/\ell^*$. For backscattering from a semi-infinite sample, this gives

$$G_1(\tau) = \exp\left(-\gamma\sqrt{\frac{6\tau}{\tau_0}+\frac{3\ell^*}{\ell_a}}\right) \qquad (8)$$

The solid lines through the data in Fig. 5 are obtained from Eq. (8) with $\ell^*$=144 $\mu$m and with

$\ell_a$=4.80 mm and 2.53 mm, respectively, for the two samples. The absorption lengths were measured in water in the absence of polystyrene spheres, so that except for an overall normalization, there are no adjustable parameters. The agreement between Eq. (8) and the data is very good.

Finite size effects are also observed in backscattering when the diameter of the exciting laser beam, $d_0$, is not large enough for the beam to be approximated as having infinite extent. This restricts the contributions of long paths to the autocorrelation function and occurs for times shorter than $\tau_0[\ell^*/(d_0/2)]^2$. Thus, care must be exercised to ensure that a beam of sufficient width and uniform intensity is used in order to apply Eq. (6) backscattering data.

In contrast to transmission, in backscattering the distance into the sample at which the light begins to diffuse plays an import role. This is evident by the strong dependence of Eq. (6) on the factor $\gamma$. Physically this suggests that the form of $G_1(\tau)$ is very sensitive to how the propagating light is converted to diffusing light in the first few scattering events. We have adopted a very simple model of this process by assuming that propagating light is converted directly to diffusing light at a single distance, $z_0=\gamma\ell^*$, inside the sample. This approximation clearly gives results which agree very well with the experiment, provided that $\gamma\approx 2$. However, the actual conversion process is much more complex and different models for how the incident light scatters in the first few steps can lead to significantly different results.

To gain insight into how $G_1(\tau)$ depends on the first few scattering events, we can modify the initial conditions for the diffusion equation. For example, to account for the spatial dependence of the initial scattering process, we could assume that $U_{in}=\exp(-z/\gamma\ell^*)\delta(t)$ instead of $U_{in}=\delta(z-z_0,t)$. In this case, the form of the autocorrelation function changes dramatically:

$$G_1(\tau) = \left[1+\gamma\sqrt{\frac{6\tau}{\tau_0}}\right]^{-1} \quad \text{for } L \gg \gamma\ell^* \qquad (9)$$

However, Eq. (9) does not fit the data, as shown in Fig. 3. Stephen has obtained a similar power law form for $G_1(\tau)$ in backscattering using diagrammatic techniques, but still within the diffusion approximation (2). Stephen's model also implicitly assumes that the spatial dependence of the conversion process is exponential. While his approach fails to describe the data at long times, for $\tau \ll \tau_0$ he finds that $G_1(\tau)\sim[1-2(\tau/\tau_0)^{1/2}]$ in agreement with the data and without the arbitrary assumption that $\gamma\approx 2$, as in our model. This suggests that the diffusion approximation works best for long light paths, that is, when $\tau \ll \tau_0$. At longer times, short paths make the dominant contribution to the decay of the autocorrelation function. These paths consist of only a few scattering events and are poorly described by the continuum approximation of light diffusion. Our approach of converting incoming beam to diffusive light several $\ell^*$ into the sample eliminates the contributions of the shortest paths. Perhaps fortuitously, this approach agrees with the data. Thus, an important remaining theoretical problem is to obtain a fundamental understanding of the experimentally observed form of $G_1(\tau)$ without arbitrary assumptions about how light enters the sample. The key to progress probably lies in obtaining a more realistic description of the shortest paths for which the diffusion approximation fails.

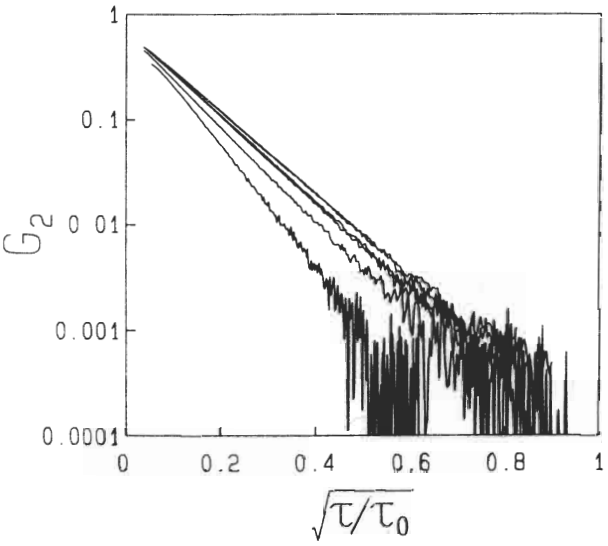


Figure 6. Intensity autocorrelation functions vs square root reduced time for backscattering from suspensions of particles with different diameters. From the lower left to the upper right corner, the curves correspond in order to data from 0.091–$\mu$m, 0.198–$\mu$m, 0.305–$\mu$m, 0.497–$\mu$m, 0.412–$\mu$m, and 0.605–$\mu$m diameter spheres

## Applications of DWS

**Particle sizing.** An important goal of extending PCS to multiple scattering regimes is the development of a simple optical technique of sizing particles. DWS now provides such a technique. To illustrate its utility, we measure autocorrelation functions in backscattering for several monodisperse colloidal suspensions with polystyrene spheres of different sizes. We use six different samples with $\phi$=0.05 and with sphere diameters $d$ ranging from 0.091 $\mu$m to 0.605 $\mu$m. In Fig. 6, we plot log $G_2(\tau)$ versus square root of reduced delay time, $\tau/\tau_0$. For $d \gtrsim 0.3$ $\mu$m, the scaled autocorrelation functions nearly all fall on a single curve. This scaling of $G_1(\tau)$ suggests that the parameter $\gamma$ approaches an asymptotic limit of ~2 for $d \gtrsim \lambda$ and that Eq. (6) can be used to determine $\tau_0=(Dk_0^2)^{-1}$. Thus, if the relationship between $D$ and $d$ is known, as is the case for small $\phi$, DWS can be used to determine particle sizes to better than 10%.

For $d \lesssim 0.3$ $\mu$m, the data can still be described by

Eq. (6), but with larger values of $\gamma$. For $d$=0.091 $\mu$m, $\gamma$=2.4 and for $d$=0.215 $\mu$m, $\gamma$=2.3. In fact, with the exception of $d$=0.412 $\mu$m, $\gamma$ increases monotonically with $d$ over the entire range of particle sizes measured. Preliminary data suggest that the size dependence of $\gamma$ is strongly dependent on the polarization of the emerging light and on the scattering anisotropy of the particles as measured by the ratio $\ell^*/\ell$. However, a detailed discussion of the effects of polarization and scattering anisotropy is beyond the scope of this paper and will be presented elsewhere.

**Mixtures.** The systems which are studied in practical applications of light scattering are often polydisperse, that is, they consist of a distribution of particle species which have different optical properties or different diffusion coefficients. In the case of conventional PCS this leads to non-exponential correlation functions which have been analyzed in a variety of ways, often in the form of cumulant expansions. The first cumulant gives an average of the diffusion coefficients, while the second cumulant gives information about the polydispersity. In the case of strong multiple scattering, the decay of the correlation function is already non-exponential and geometry dependent, but should there be additional changes in the time dependence of the autocorrelation function? The essence of our ability to calculate the correlation function was the idea that the light path through a sample consisted of a random walk of phase shifts caused by the motion of the individual particles along the scattering path. In the diffusion approximation, the statistics of random walks reduce to simple Gaussian functions. If we let the step size of a random walk vary for each step, the statistics remain the same in the large n region as for a single step size walk with an average step size. This is a result of the central limit theorem. Thus, if we can use the diffusion approximation at all, the time dependence of the autocorrelation function should be the same for a polydisperse system as a monodisperse one. Therefore, in DWS all information about polydispersity is contained in the absolute value of the average diffusion coefficient, and not in the shape of the autocorrelation function, as in PCS. The question which remains is how to calculate the appropriate average diffusion coefficient for a polydisperse sample.

We limit our discussion here to the case of non-interacting particles. For simplicity, we first consider the case of a bimodal distribution of particles with number density $\rho_i$, scattering cross section $\sigma_i$, and diffusion coefficient $D_i$, with $i$=a,b. To calculate the autocorrelation function, we again start from Eq. (1) and consider a single light path. Rewriting Eq. (1b) to explicitly account for the two species of particles gives

$$\Delta\phi(\tau)=\sum_{i=1}^{n_a} \boldsymbol{q}_a \cdot \Delta \boldsymbol{r}_a(\tau) + \sum_{i=1}^{n_b} \boldsymbol{q}_b \cdot \Delta \boldsymbol{r}_b(\tau)$$

We again use the statistical independence of $\boldsymbol{q}_i$ and $\boldsymbol{r}_i$ and of each individual scattering event in the path, but recognize that in general $\langle q_a^2\rangle \neq \langle q_b^2\rangle$. Thus, upon averaging we obtain

$$G_1(\tau) \approx e^{-\delta\phi^2(\tau)} \tag{10a}$$

where

$$\delta\phi^2(\tau) \equiv \{\langle q_a^2\rangle \langle \Delta r_a^2(\tau)\rangle n_a + \langle q_b^2\rangle \langle \Delta r_b^2(\tau)\rangle n_b\}/6 \tag{10b}$$

where in averaging over $\boldsymbol{q}$ we again keep only the first term in a cumulant expansion. The averages in Eq. (10b) are given by $\langle q_a^2\rangle = 2k_0^2(\ell_a/\ell_a^*)$ and $\langle \Delta r_a^2(\tau)\rangle = 6D_a\tau$ and similarly for b. Thus:

$$\delta\phi^2(\tau) \equiv 2k_0^2[D_a(\ell_a/\ell_a^*)n_a + D_b(\ell_b/\ell_b^*)n_b] \tag{11}$$

The problem which remains is to determine the average number of scattering events from particle species a and b in a path of total length s. The relative probabilities of scattering by species a and b are proportional to their number densities and scattering cross sections or inversely proportional to their individual mean free paths:

$$n_a/n_b = (\rho_a\sigma_a/\rho_b\sigma_b) = \ell_b/\ell_a$$

or $n_a\ell_a = n_b\ell_b$. Substitution into Eq. (11) gives

$$\delta\phi^2(\tau) = 2k_0^2 n_a\ell_a[D_a/\ell_a^* + D_b/\ell_b^*].$$

The total path length is given by $n$ steps with the actual mean free path of the system $\ell'$ which includes scattering from both species:

$$1/\ell' = \rho_a\sigma_a + \rho_b\sigma_b = 1/\ell_a + 1/\ell_b$$

where $s = n\ell' = n_a\ell_a$ since $n = n_a + n_b = n(1+\ell_a/\ell_b)$. The final result for decay of the autocorrelation function along a single path is

$$G_1(\tau) = \exp\{-2k_0^2(D_a/\ell^*_a + D_b/\ell^*_b)\tau s\}$$

The dependence on $s$ and $\tau$ is the same as in Eq. (3) which was used in deriving the expressions for $G_1(\tau)$ for multiple scattering in different geometries. As suggested at the beginning of this section the time dependence of the correlation functions will therefore not change from the results for a single species; we must merely substitute the appropriate averages for $\ell^*$ and $\tau_0$. Writing the mean square phase shift as

$$\delta\phi^2(\tau) = 2(\tau/\tau_{eff})(s/\ell_{eff})$$

and generalizing to the case of many different species we have

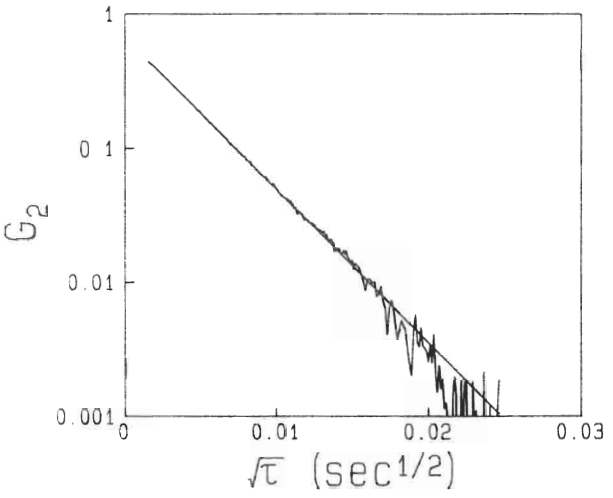


Figure 7. Intensity autocorrelation function vs square root time for backscattering from a mixture with 0.198–$\mu$m spheres at 2 vol.% and 0.605–$\mu$m spheres at 2 vol.%.

$$1/\ell^*_{\text{eff}} = \Sigma_j 1/\ell^*_j \tag{12a}$$

$$1/\tau_{\text{eff}} = D_{\text{eff}} k_0^2 \tag{12b}$$

$$D_{\text{eff}} = (\Sigma_j D_j/\ell^*_j)/(\Sigma_j 1/\ell^*_j) \tag{12c}$$

Thus, the effective diffusion coefficient is just the weighted average of the diffusion coefficients where the weighting factor is the density times the transport cross section, or alternatively, the inverse transport mean free path. The expressions for $\tau_{\text{eff}}$ and $\ell^*_{\text{eff}}$ can be directly substituted for $\tau_0$ and $\ell^*$ in the correlation functions previously derived.

To test these ideas we measure $G_2(\tau)$ in transmission and backscattering for several mixtures of 0.198-$\mu$m and 0.605-$\mu$m diameter spheres in water. In Fig. 7 we show $G_2(\tau)$ obtained in backscattering with $\phi_a$=0.02 for the 0.198-$\mu$m spheres and $\phi_b$=0.02 for the 0.605-$\mu$m spheres. The data are well described by the functional form given in Eq. (6) and decay exponentially with the square root of time, as expected. Similarly, data obtained using a point source in transmission follow the functional form given in Eq. (5).

To make quantitative comparisons between theory and experiment, we calculate $\ell_a^* = [\rho_a \sigma_a \langle 1-\cos\theta_a \rangle]^{-1}$ and $\ell_b^* = [\rho_b \sigma_b \langle 1-\cos\theta_b \rangle]^{-1}$ from Mie theory. Then, using the Stokes-Einstein equation to calculate the diffusion coefficient for each species, we calculate $\tau_{\text{eff}}$ using Eq. (12). In Fig. 8 we compare $\tau_{\text{eff}}$ calculated using this procedure to backscattering measurements of $\tau_{\text{eff}}$ for different mixtures of 0.198-$\mu$m and 0.605-$\mu$m diameter spheres. The agreement between theory and experiment is excellent. Similar agreement between theory and experiment was also found for transmission data.

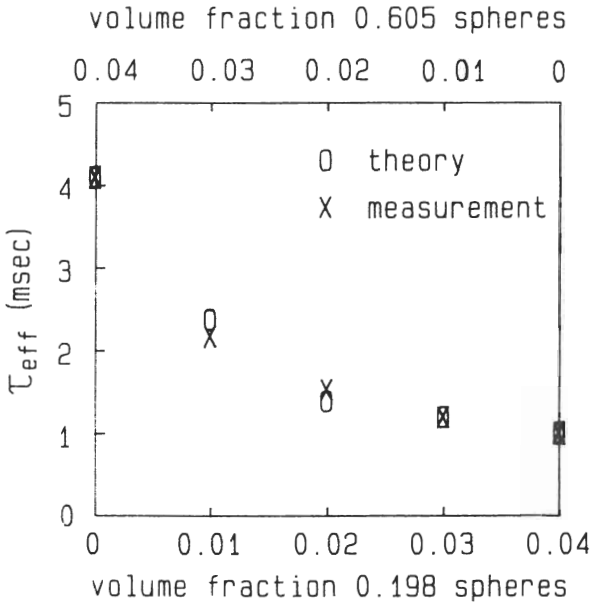


Figure 8. Effective decay time $\tau_{\text{eff}}$ vs volume fraction $\phi$ for mixtures of 0.198–$\mu$m and 0.605–$\mu$m spheres.

## Conclusions

In this paper, we have demonstrated a simple method for quantitatively interpreting PCS data from optically dense systems. We exploit the diffusive nature of the transport of light in multiply-scattering media, and obtain expressions for the temporal autocorrelation functions. Excellent agreement with the data is obtained for a wide variety of experimental conditions, and we are able to account for the effects of scattering geometry, sample geometry, absorption, and polydispersity.

By comparison to conventional PCS, the decay rate of the autocorrelation function in DWS is considerably faster, since the decay is due to the cumulative effect of many scattering events. As a consequence, much smaller motions of the individual particles, $\Delta r_{\text{rms}}$, can be probed. In the transmission geometry, the sample thickness $L$ sets the dominant length for the light paths so that particle motion is probed over a narrow range of length scales around $\Delta r_{\text{rms}} \sim \lambda \ell^*/(4L)$. Thus, by varying the sample thickness, this range of length scales can be experimentally adjusted. By contrast, the backscattering geometry probes motion over all length scales smaller than the wavelength, since light paths of all lengths are possible. In the freely diffusing systems discussed in this paper, these length scales correspond directly to time scales set by the diffusion coefficient of the particles. However, in many dense systems which exhibit multiple scattering, particle interactions cause the diffusion coefficient to be time dependent. In these systems DWS becomes a particularly powerful probe of the time dependence of $\Delta r_{\text{rms}}$. Thus,

optically dense colloids, gels, and other macromolecular systems previously difficult or impossible to study with conventional PCS should provide fertile problems for study with DWS.

**Acknowledgements**

We thank G. Maret, P.E. Wolf, and M.J. Stephen for stimulating discussions and important preprints.

**References**

1. G. Maret and P.E. Wolf, "Multiple scattering from disordered media. The effect of Brownian motion of scatterers," Z. Phys. B **65**, 409-413 (1987).
2. M.J. Stephen, "Temporal fluctuations in wave propagation in random media," Phys. Rev. B **37**, 1–5 (1988).
3. D.J. Pine, D.A. Weitz, P.M. Chaikin, E. Herbolzheimer, "Diffusing Wave Spectroscopy," Phys. Rev. Lett. **60**, 1134-1137 (1988).
4. H.S. Carslaw and J.C. Jaeger, *Conduction of Heat in Solids, second edition* (Oxford University Press, 1959).
5. H.C. van de Hulst, *Light Scattering by Small Particles* (Dover, New York, 1981).
6. E. Akkermans, P.E. Wolf, R. Maynard, and G. Maret, "Theoretical study of the coherent backscattering of light by disordered media," J. Phys. France **49**, 77–98 (1988).
7. M.P. van Albada and A. Lagendijk, "Observation of weak localization of light in a random medium," Phys. Rev. Lett. **55**, 2692-2695 (1985); P.E. Wolf and G. Maret, "Weak localization and coherent backscattering of photons in disordered media," Phys. Rev. Lett. **55**, 2696–2699 (1985).
8. P.E. Wolf, G. Maret, E. Akkermans, and R. Maynard, "Opical coherent backscattering by random media: an experimental study," J. Phys. France **49**, 77–98 (1988).